

# In Silico Docking Analysis of Rat $\gamma$ -Crystallin Surfaces

Alaa El-Din A. Gawad<sup>1</sup>

## Abstract

In *silico* methods are useful for predicting 3D structure of binding sites when experimental information is lack. The complex interaction between  $\gamma$ -crystallins and small ligands is a key element in understanding the lens transparency. In spite of the high sequence similarity of  $\gamma$ -crystallins, different numbers of pockets were automatically identified on their molecular surfaces.  $\gamma$ C-crystallin has the largest binding pocket among rat  $\gamma$ -crystallin individuals. The binding affinities of five putative chemical ligands against the active sites of  $\gamma$ -crystallin proteins were determined by Autodock 4.2. Molecular docking indicated multiple binding modes of such ligands into  $\gamma$ -crystallins pockets.

**Keywords:**  $\gamma$ -crystallin family, rat, binding sites, molecular docking, monosacchrides, aspirin, ibuprofen, vitamin C

---

<sup>1</sup> Biophysics and Laser Sciences Unit, Research Institute of Ophthalmology, Giza, EGYPT, e-mail: alaael\_din3@hotmail.com

## 1 Introduction

$\gamma$ -Crystallins are lens water-soluble proteins present in major classes of vertebrates except the birds and reptiles (Wistow and Piatigorsky 1988). It accounts for 40% of the total protein mass in rat and mouse (Oken *et al.*, 1977; Wada *et al.*, 1981). It is composed of at least seven monomeric proteins ( $\gamma$ A- $\gamma$ F and  $\gamma$ S) with only  $\gamma$ A-,  $\gamma$ B-,  $\gamma$ C-,  $\gamma$ D-, and  $\gamma$ S present in human (Bloemendal *et al.*, 2004). They show a high degree of sequence homology (D'Alessio, 2002). Nevertheless, they have slight differences in the net charge and are immunologically heterogeneous (Alaa, 2009; Vornhagen *et al.*, 1982). Expression of  $\gamma$ -crystallin genes shows differential decrease post-natally and in mature rat lens only  $\gamma$ B-crystallin can be detected (Siezen *et al.*, 1988). Moreover,  $\gamma$ -crystallins are markers of the terminally differentiated lens fiber cells. However, it has been reported that some  $\beta$ - and  $\gamma$ -crystallin components were found in lens epithelial cells (Wang *et al.*, 2004). Further,  $\gamma$ -crystallins present in murine retinas (Sinha *et al.*, 1998, Jones *et al.*, 1999, Xi *et al.*, 2003).

The  $\gamma$ -crystallins are made up of so-called modified Greek key motifs that intercalate to form highly symmetrical two domains (Slingsby and Clout, 1999). Interestingly, although the overall electrostatic surface potential maps of  $\gamma$ -crystallins are rather similar, the molecular interaction field of these proteins is different (Alaa, 2009). In principle, the biophysical basis for transparency of the eye lens is closely linked to the unique structure and function of lens proteins. In this context, as the lens ages, the crystallins also age which may result in senescence cataract. Age-related cataract is likely to reflect altered state of solubility and protein-protein interactions of lens crystallins (Ma *et al.*, 1998, Pande *et al.*, 2010, Sakthivel *et al.*, 2010). Therefore, understanding the networks of molecular interactions between  $\gamma$ -crystallin proteins and small ligands is crucial for the prediction of biochemical functions. Moreover, the knowledge of all relevant surface characteristics and binding sites in protein molecules is of utmost

importance. Fan *et al.* (2004) reported that mouse  $\gamma$ E- and  $\gamma$ F-crystallins are specifically able to interact with MIP.

The principal function of lens crystallins is to focus light onto the retina to enable an image to be seen. It is likely that lens crystallins have diverse functions in and outside the eye (Piatigorsky, 1998, Andley, 2007). On one hand,  $\alpha$ -crystallin is reported to be essential for maintaining the integrity of the cytoskeleton, and prevent apoptosis both in vitro and in vivo (Horwitz, 2003). On the other hand, little is known about the non-refractive roles of the  $\beta$ - and  $\gamma$ -crystallins. The defective  $\gamma$ -crystallin gene expression leads to certain types of hereditary cataracts in mice and humans (Graw, 2003). The various  $\gamma$ -crystallin mutations show morphologically distinct phenotypes. Furthermore, multiple mutations for a single  $\gamma$ -crystallin gene have heterogeneous phenotypes that indicate distinct functions of the individual  $\gamma$ -crystallins (Graw 2003).

In this work, a detailed study of the rat  $\gamma$ -crystallin surfaces has been carried out to get insight into the putative binding sites and biological interactions. Hypothetical  $\gamma$ -crystallin models corroborated the differential binding of multiple ligands, monosaccharides, aspirin, ibuprofen and vitamin C. Computer aided ligand docking was carried out using the automated Autodock4.2 program, and potential ligands were selected out based on their chemical complementarity and steric fit within the binding site of the rat  $\gamma$ -crystallins. This technique can predict the different bound ligand conformations in absence of the results from conventional techniques.

## 2 Materials and Methods

The 3D homology models of rat  $\gamma$ -crystallins were generated with Modeller 9V7 (Eswar et al., 2003; Sali and Blundell, 1993) by using the X-ray crystal structure of bovine  $\gamma$ B-crystallin (1AMM) and bovine  $\gamma$ F-crystallin (1A45) as

templates. Details of these models have been described previously (Alaa, 2009).

## 2.1 Binding sites identification

The search for common putative surface binding sites on  $\gamma$ -crystallin proteins was performed applying a probe radius of 1.4 Å in the CASTp (Computed Atlas of Surface Topography of proteins) server (Dundas *et al.*, 2006). In addition, the researcher wanted to use another approach to check the reliability of the results. For this purpose, Q-SiteFinder program (Alasdair *et al.*, 2005) in which the pockets are defined by binding hydrophobic (-CH<sub>3</sub>) probes to the protein and finding clusters of probes with the most favorable binding energy was employed. Each pocket is assigned a unique identification number, roughly corresponding in order of increasing volume.

## 2.2 Automated docking simulation

Small ligands, ascorbic acid, aspirin, fructose, and  $\beta$ -D-glucopyranose, and ibuprofen, have been used to explore the obtained pockets of proteins as they form well-known protein-ligand complexes for which no binding mode is yet structurally determined.

$\gamma$ -Crystallin models were prepared for docking in AutoDockTools suite (version 1.4.5); polar hydrogen atoms were added to the structures, and Gasteiger and Kollman united atom charges were used for the ligand and protein atoms, respectively. In the current study, the proteins are considered as rigid bodies while the ligand is free to rotate, translate and change conformation during the docking application. The entire protein surfaces were subjected to blind docking simulations using the Lamarckian genetic algorithm (LGA) and the Solis & Wets local search method of Autodock 4.2 program (Morris *et al.*, 1998). The

AutoDock program could select the correct protein-ligand complexes based on the binding free-energy (Hetényi and van der Spoel, 2002; Huey et al., 2006). A population size of 150 and 2,500,000 energy evaluations were used for 100 search runs. The docking area was defined by a box, with grid spacing of 0.375 Å and the dimension of 90x90x120 points along the x, y and z axes. AutoGrid and AutoDock were used for calculation of grid maps and docking, respectively. The docking results from each of the 100 calculations were ranked according to the binding free energy. Ten conformations for each substrate were obtained. A 2.0 Å tolerance was used to form clusters of the closest structures. The best conformations were selected on the basis of combination of binding energies as well as location of the docking.

### **3 Main Results**

#### **3.1 Determination of $\gamma$ -Crystallin Pockets**

The search for pockets on  $\gamma$ -crystallin protein surfaces was performed using CASTp (Binkowski *et al.*, 2003) server. CASTp server used weighted Delaunay triangulation and the alpha complex for shape measurements. CASTp is designed for identifying and characterizing protein surface accessible pockets, functional residues located on protein surface and voids buried under the interior of proteins by measuring concave surface regions of three dimensional structures of proteins. The number and total volume of pockets and cavities in the rat  $\gamma$ -crystallin proteins vary widely among the models and bovine  $\gamma$ B- and  $\gamma$ F-crystallins (reference structures) as well (Table 1). In addition, there is quite variation in the number of pocket mouths and the area of mouth openings. However, both CASTp and Q-SiteFinder show that  $\gamma$ C-crystallin has the largest calculated internal cavity surface volume. Close inspection of the predicted pockets displaying the surface of some potential pockets are lined with hydrophilic amino acid residues ( $\gamma$ B-,  $\gamma$ D-,

and  $\gamma$ F-crystallins) whilst  $\gamma$ D-, and  $\gamma$ E-crystallin surface harbors a hydrophobic binding pockets (Table 2 supplement). Indeed, there exist networks of interconnected pockets.  $\gamma$ A-crystallin gets a single network of pockets encompasses most the entire space between the two the domains (Figure 1, panel A).  $\gamma$ B-,  $\gamma$ C- and  $\gamma$ E-crystallins displayed two networks; one network in the loop connecting the two domains and the other between the two domains (Figure 1, panels B, C, E). On the first domain surface of  $\gamma$ D- and  $\gamma$ F-crystallins, an additional network has been predicted (Figure 1, panels D&F). The small ligand molecules such as aspirin, ascorbic acid, glucose, fructose, and ibuprofen, have been used to probe the 3D space of the binding sites for  $\gamma$ -crystallins.

## 3.2 In Silico Docking

The feasibility of the predicted binding pockets in the protein models was assessed by blind docking methodology, which does not require any a priori knowledge about the location of the binding sites or function of the protein. If the active ligands docked into predicted pockets of the protein models, this conforms the predicted pockets to be binding sites. From the clustering procedure in Autodock, multiple docking sites on substrate proteins are predicted to occur in *in silico* docking experiments for each ligand molecule. Surprisingly, these small ligands showed a common binding site for  $\gamma$ A-,  $\gamma$ C-,  $\gamma$ D-, and  $\gamma$ E-crystallins; common binding pocket for aspirin, fructose, glucose, and ascorbic acid exists in  $\gamma$ B-crystallin whereas  $\gamma$ F-crystallin has a common binding pocket for aspirin, glucose, ibuprofen, and ascorbic acid (Table 3). It has been concentrated on binding modes that present the lowest energy conformation.

### 3.2.1 Docking of Monosaccharides

When docking the fructose on the  $\gamma$ -crystallins, the calculated binding energy

and calculated  $K_i$  predicted by docking showed that fructose- $\gamma$ A-crystallin complex has the highest binding energy, followed by  $\gamma$ C-,  $\gamma$ D-,  $\gamma$ E-,  $\gamma$ B-, and  $\gamma$ F-crystallins, respectively. In addition, the binding affinity of fructose to  $\gamma$ A-crystallin is ~8-fold higher than that of the  $\gamma$ F-crystallin (Table 4). Although the primary structure of  $\gamma$ -crystallins is highly conserved, the pockets are composed of a variety of amino acid residue types (both polar and hydrophobic) (Table 4).

Conversely, glucose showed high binding affinity to  $\gamma$ D-crystallin (137  $\mu$ M) and then  $\gamma$ F-,  $\gamma$ B-,  $\gamma$ E-,  $\gamma$ C-, and  $\gamma$ A-crystallins (Table 5). The amino acid sequences of glucose-binding pockets are highly similar except for  $\gamma$ D-crystallin. Tables 4 and 5 show that the binding energy of  $\gamma$ -crystallin-fructose complex is more stable than the corresponding energy  $\gamma$ -crystallin-glucose complex except for  $\gamma$ D-crystallin.

The docking results were further analyzed counting the number of hydrogen bonds occurring between docked conformers and amino acids of  $\gamma$ -crystallins (Table 4). Tyr-46 residue of  $\gamma$ A- and  $\gamma$ E-crystallins forms hydrogen bonds with C-3 of fructose molecule. Arg-80 (HH11 and HH21 atoms) and HH12 atom of both  $\gamma$ A- and  $\gamma$ E-crystallins forms hydrogen bonds with C-5, C-6 and C-4 respectively while Arg-147 residue of  $\gamma$ A (HN)- and  $\gamma$ E (HE)-crystallins creates a hydrogen bond with C-1 and C-6 of fructose, respectively. In  $\gamma$ B-, and  $\gamma$ C-crystallins, Gln-55 (HN) hydrogen bonding to C-6 while in  $\gamma$ E (OE1 and HE22)-crystallin it binds to C-3 and C-2 of fructose, respectively. HN atom of Gln-144/143 residue in  $\gamma$ B-,  $\gamma$ C- and  $\gamma$ D-crystallins creates a hydrogen bond with C-6 and C-1 atoms of fructose, respectively (Figure 2).

Docking experiments confirmed that glucose is anchored to a carbohydrate-binding site (pocket) through a network of 5-7 hydrogen bonds in  $\gamma$ -crystallins (Table 5). Judging from the docking models, Phe-57 in  $\gamma$ A- and  $\gamma$ B-crystallins displayed hydrogen bonds with C-2 and C-3 of glucose, respectively. Hydrogen atoms of C-3 and C-2 of glucose bind to carboxylic

oxygen in D-62 in  $\gamma$ C-, and  $\gamma$ E-crystallins. Gln-68 forms a single hydrogen bond with C-1 of glucose in  $\gamma$ A- and  $\gamma$ B-crystallins while in  $\gamma$ C-crystallin it creates a network of hydrogen bonds with C-1, C-2 and C-3 of glucose and C-3 and C-4 in  $\gamma$ E-crystallin. Furthermore, the hydrogen bond of Tyr-134/135 in  $\gamma$ A-,  $\gamma$ B-, and  $\gamma$ F-crystallins binds C-4 and C-6 in glucose, respectively. Also, OE1 atom of Gln-143/144 in  $\gamma$ A-,  $\gamma$ B-, and  $\gamma$ F-crystallins binds oxygen of C-1 for glucose. Arg-169/168 in  $\gamma$ B-,  $\gamma$ F-crystallins is sharing its HH21 with oxygen in C-6 and C-3 of glucose, respectively (Figure 3).

### 3.2.2 Docking of Aspirin, Ibuprofen and Vitamin C

The analgesic and anti-inflammatory agents and the antioxidant studied in this work include aspirin, ibuprofen, and Vitamin C. These drugs are selected because they have been subjects of extensive investigation including the probing of toxicity and side effect protein targets of these drugs. Comparative docking of  $\gamma$ -crystallins with the aspirin, ibuprofen and ascorbic acid revealed that the binding affinity of ibuprofen is the highest against  $\gamma$ -crystallins (Table 7).

#### 3.2.2.1 Aspirin

The resulting models for binding of aspirin on the  $\gamma$ -crystallin proteins are displayed in Figure 4 and, the list of contacting residues (up to 4Å) is given in Table 6.  $\gamma$ -Crystallins showed different binding preferences. For example,  $\gamma$ F-crystallin has ~5.2-fold lower affinity than  $\gamma$ B-crystallin. Aspirin binds with  $\gamma$ -crystallin proteins by different number of hydrogen bonds (Table 6). There are no common residues involved in the formation of van der Waals, electrostatic and hydrophobic interactions (Table 6). In  $\gamma$ A-crystallin a double hydrogen bond was formed from the oxygen of carboxylic group of aspirin, both to HH11 and HH21 in aminoacetal of Arg-80. Another hydrogen bond extends from hydroxyl group of Tyr-151 to ligand's oxygen of oxyacetyl group. In  $\gamma$ B- and  $\gamma$ C-crystallins, the

oxygen of ligand's hydroxyl group is hydrogen bonded to HH21, H11, H12 and HH22 in aminoacetal of Arg-80 and Arg-147/148 respectively. In both  $\gamma$ C- and  $\gamma$ F-crystallins, oxygen of oxyacetyl group of ligand forms hydrogen bonds with HE21 and HN of Gln-55 respectively. In  $\gamma$ D-crystallin, phenolic oxygen, oxygen of acetoxyl group and oxygen of –OH group of ligand forms hydrogen bonds with HN, HE and HH22 of Arg-59. In  $\gamma$ E-crystallin, both oxygen of –OH group and carboxylic oxygen of ligand forms hydrogen bonds with HG and HN of Ser-84. In contrast, HD atom of His-83 extends to bind oxygen of phenolic group in Aspirin.

### 3.2.2.2 Ibuprofen

Comparative docking of rat  $\gamma$ -crystallins with the ibuprofen revealed that the amino acid sequence of  $\gamma$ C- and  $\gamma$ D-crystallins is largely similar (Table 7). While the binding energy difference between  $\gamma$ F-crystallin-ibuprofen complex and  $\gamma$ E-crystallin-ibuprofen complex is about 1.75 Kcal/mol, the inhibition constant ( $K_i$ ) of ibuprofen is ~19 times less for the latter. Oxygen of carboxylic group of ibuprofen has a bi-dentate hydrogen bonding interaction with HH11 atom in both Arg-80 and Arg-147 in  $\gamma$ A-crystallin (Figure 5). In  $\gamma$ B- and  $\gamma$ F-crystallins, HH21 atom of the side chain of Arg-169/168 residue forms the hydrogen bonds with oxygen of hydroxyl group of the ligand, while HH22 atom of Arg-168 in  $\gamma$ E-crystallin binds oxygen of the carbonyl group (Figure 5). However, the oxygen of hydroxyl group of ibuprofen is sharing the hydrogen bond with HN of both Gln-55 and Gln-143 in  $\gamma$ C- and  $\gamma$ D-crystallins (Figure 5).

### 3.2.2.3 Vitamin C

The binding energy results showed that vitamin C binds with  $\gamma$ -crystallins in the order of  $\gamma$ C >  $\gamma$ A >  $\gamma$ D >  $\gamma$ B >  $\gamma$ F >  $\gamma$ E (Table 8). The docking results revealed that the binding mode of vitamin C is similar for  $\gamma$ B- and  $\gamma$ C-crystallins. Figure 6 displays the interaction of  $\gamma$ -crystallins and vitamin C. In  $\gamma$ B- and  $\gamma$ C-crystallins the carboxylic oxygen of Asn-50 residue forms hydrogen bond with C-1 and C-6

of ligand, respectively. The hydrogen atoms (HH11 and HH22) of Arg-80 residue in  $\gamma$ A- and  $\gamma$ C-crystallins bonded with O4, while in  $\gamma$ B- (HH21 atom) and  $\gamma$ C-crystallin (HH12 atom) bind with O5 of ascorbic acid. The oxygen atom of carbonyl group of Leu145 residue in  $\gamma$ A-crystallin makes bifurcated hydrogen bonds with C-2 and C-3 of ascorbic acid and Leu 146/145 residue in  $\gamma$ B- and  $\gamma$ C-crystallins form hydrogen bond with O2 of ascorbic acid. Arg-147/148 residue in  $\gamma$ A-,  $\gamma$ B-, and  $\gamma$ C-crystallins showed hydrogen bonds with O1 and O5, respectively. The carboxylic oxygen atom in both Phe-57 and Y-134 residues of  $\gamma$ D-, and  $\gamma$ E-crystallins binds the hydrogen bonded O5, O2, and O1, respectively. These are the main results of the paper.

## 4 Discussion

The absence of the X-ray crystallography for the interaction between small ligands and lens proteins may thwart the inference of biochemical protein function and the development of rational drugs. However, assignment the potential binding sites of a protein on the basis of biophysical information, for instance molecular surface geometry and electrostatic surface potential similarities, employing docking methodology represents an elegant solution. The binding sites of  $\gamma$ -crystallins are composed of contiguous pockets (Figure 1). These pockets vary greatly in shape and size, from minor indentations between surface atoms to large cavities between protein domains. In general, it has been suggested that ligand binding sites involve the largest pockets (Laskowski et al., 1996 and Liang et al., 1998). It has also been reported that pockets show greater variation in their shapes than can be accounted for by the conformational variability of the ligand (Kahraman et al., 2007).

Glycation is a slow process under physiological conditions, and is thought a pivotal factor in the pathogenesis of diabetic cataract (Monnier and Cerami,

1982; Lyons et al., 1991; Lal et al., 1995). In rat  $\gamma$ -crystallin models, the position occupied by the main key residues involved in ligand binding (see *Figs. 2, 3, 4, 5 and 6*) is similar to the available experimental data (Smith et al. 1996 and Yan et al., 2003). However, these sequences represent the primary structure of those proteins. Hence, docking simulation was carried out to predict the most favorable conformation of fructose and glucose (the one with the lowest docked energy). In addition, the binding pocket structure is almost invariably linked with the relative arrangement of atoms (3D) forming the amino acid residues of the primary structure.

The docked ligands fit well into the binding pockets and show a variable number of hydrogen bonds in each protein substrate. The binding sites showed a more fructose preference than glucose for all  $\gamma$ -crystallins (Tables 4 and 5). It has been reported that the binding sites are enriched in aromatic (His, Phe, Tyr, Trp) residues provides the hydrophobic platform common to carbohydrate–protein interactions, and depleted in charged residues (Asp, Glu, Lys) with the exception of arginine (Brás et al., 2009 and Leis et al., 2010). Incubation of  $\gamma$ -crystallins in vitro with either fructose or glucose showed the glycation by fructose proceeds at an accelerated rate compared with the same concentration of glucose (*Kawasaki et al., 1998*). In  $\gamma$ E-crystallin, the ligand binding pocket for both fructose and glucose is the same. However, the side-chains of amino acid residues form different hydrogen numbers with multiple diverse ligands (Figures. 2E and 3E).

$\gamma$ -Crystallins are reported almost equivalent to the other crystallins as a substrate for glycation by ascorbic acid (Swamy and Abraham, 1991). Despite the close sequence homology of the binding sites for  $\gamma$ A-,  $\gamma$ B-, and  $\gamma$ C-crystallins, the affinity of ascorbic acid to  $\gamma$ C-crystallin is the highest. It seems likely that the relative rotation of ascorbic acid ligand in respect to amino acid residues forming the binding site giving rise to the formation of hydrogen bonds (Table 8 and Figure 6). However, it has been found that the incorporation of ascorbic acid, in vitro, into lens proteins is concentration dependent and 18-fold rapidly than

glucose on a molar basis (Lee et al., 1998).

Ibuprofen, non-steroidal anti-inflammatory drugs (NSAIDs) and aspirin possess anti-cataract potential (Shyadehi and Harding, 1991; Yan et al., 2008). It has been found that aspirin alone or in combination with carnosine reduces glycation in vitro, and in animal experiments, probably by acetylation of amino groups while ibuprofen can bind non-covalently to the proteins (Ajiboye and Harding, 1989, Roberts and Harding, 1990, Shi et al., 2009). Docking experiments has shown that only  $\gamma$ B-crystallin has a common binding site for both aspirin and ibuprofen. Surprisingly, in both  $\gamma$ A-and  $\gamma$ C-crystallins ibuprofen shares their binding site with glucose, while  $\gamma$ D-crystallins has a common binding site for both ibuprofen and fructose. Aspirin in both  $\gamma$ C- and  $\gamma$ D-crystallins has a common binding site for fructose and glucose respectively. In  $\gamma$ B-crystallin, Fructose, aspirin and ibuprofen have a common binding site while for  $\gamma$ E-crystallin, glucose and fructose bind the same site of aspirin.

Table 1: Comparison of the pockets detected in CASTp calculations showing pockets and cavities in rat  $\gamma$ -crystallin family

Pocket	$\gamma$ A-Crystallin		$\gamma$ B-Crystallin		$\gamma$ C-Crystallin		$\gamma$ D-Crystallin		$\gamma$ E-Crystallin		$\gamma$ F-Crystallin	
	Volume <sup>a</sup>	Area <sup>b</sup>	Volume	Area								
24	132.9	135.7									175.0	143.1
23	188.7	141.9									129.1	97.6
22	171.4	114.2			340.1	209.9					101.7	126.6
21	81.6	93.6	164.3	159.4	135.1	149.3					88.7	116.8
20	70.8	73.6	147.8	136.3	141.6	179.6	270.0	324.0			128.5	131.7
19	58.0	53.7	109.6	108.6	83.4	86.4	128.6	141.4			54.5	82.6
18	40.5	62.0	80.8	86.1	86.1	116.8	154.3	138.1			52.5	73.8
17	37.9	59.5	81.7	109.8	47.4	47.5	84.6	111.3			76.2	44.3
16	34.2	55.5	116.4	69.8	52.4	60.9	69.0	98.2			20.3	38.7
15	17.8	34.2	51.9	66.3	61.3	90.0	39.6	52.1	143.8	160.0	11.4	18.9
14	26.6	46.3	26.7	33.1	56.8	61.5	54.0	46.3	127.7	157.5	29.0	61.9
13	24.2	38.8	28.8	33.6	46.4	43.5	14.2	20.6	81.8	112.5	16.0	31.6
12	19.8	37.2	29.4	38.4	27.7	59.4	47.0	37.2	113.8	93.0	21.1	41.1
11	19.9	36.1	29.5	50.0	26.8	44.3	22.3	25.2	86.8	112.3	16.8	32.1
10	10.9	22.7	19.6	27.0	18.0	36.7	20.4	37.6	40.3	54.6	20.2	36.9
9	19.7	37.3	17.2	32.4	13.9	15.9	24.2	41.5	69.9	50.5	13.8	13.7
8	15.6	30.3	19.1	31.2	13.7	28.1	18.8	32.4	33.0	52.5	13.6	27.7
7	12.1	22.2	15.6	31.3	11.0	19.9	21.5	39.5	20.0	28.4	13.7	27.9
6	11.1	21.7	19.2	36.6	14.0	32.8	23.0	42.7	14.7	29.2	12.9	27.1
5	14.8	29.7	19.0	37.1	14.3	29.6	6.1	6.2	18.0	15.4	12.8	26.6
4	18.1	26.1	8.9	15.3	12.0	25.5	5.0	3.4	8.5	14.8	13.2	27.0
3	12.2	22.1	16.2	32.1	11.7	25.2	11.5	20.7	17.9	33.6	13.0	26.9
2	16.7	26.5	6.0	12.7	12.3	25.9	7.9	15.4	12.2	25.7	3.7	7.3
1	13.2	28.3	6.4	10.8	13.6	28.0	7.4	14.9	11.5	24.6	11.5	24.7

<sup>a</sup> Volume in  $\text{\AA}^3$       <sup>b</sup> Area in  $\text{\AA}^2$

Table 2: CASTp calculations of pockets and cavities of  $\gamma$ -crystallins

$\gamma$ A-crystallin		$\gamma$ B-crystallin		$\gamma$ C-crystallin		$\gamma$ D-crystallin		$\gamma$ E-crystallin		$\gamma$ F-crystallin	
hydrophilic	hydrophobic	hydrophilic	hydrophobic	hydrophilic	hydrophobic	hydrophilic	hydrophobic	hydrophilic	hydrophobic	hydrophilic	hydrophobic
<b>Pocket 24</b>		<b>Pocket 21</b>		<b>Pocket 22</b>		<b>Pocket 20</b>		<b>Pocket 15</b>		<b>Pocket 24</b>	
Glu 94 Ser 103 Arg 117 Glu 120	Leu 92 Tyr 93 Leu 101 Val 102 Phe 116 Leu 118 Ile 121	His 54 Gln 55 Arg 141 Arg 143 Gln 144	Glv 53 Tyr 56 Met 70 Tvr 135 Tyr 140 Glv 142 Tvr 145	Ser 40 Cvs 42 Arg 60 His 84 Thr 85 His 88 Asp 172	Met 1 Glv 41 Leu 81 Ile 82 Pro 83 Val 170 Val 171 Tvr 174	Glu 94 Gln 101 Cvs 109 Glu 120	Leu 92 Tyr 93 Met 102 Val 103 Phe 105 Leu 112 Phe 116 Phe 118 Ile 121 Va 164 Leu 167	Cvs53 Gln54 Arg 142 Gln 143	Phe 50 Thr 51 Glv 52 Tvr 55 Met 69 Phe 71 Glv141 Tvr 144 Glv 158	Arg 59 Gln 68 Gln 143 Arg 168	Phe 57 Leu 58 Tvr 63 Trp 69 Met 70 Tvr 134 Tvr 139
<b>Pocket 23</b>		<b>Pocket 20</b>		<b>Pocket 21</b>		<b>Pocket 19</b>		<b>Pocket 14</b>		<b>Pocket 23</b>	
Gln 52 Gln 55 Arg 80 Arg 147 Asp 156	Tyr 46 Tyr 51 Gly 53 Tyr 144 Leu 145 Tyr 151 Trp 157 Gly 158	Ser 40 Cys 42 Gln 84 Asp 173	Met 1 Gly 2 Gly 41 Leu 81 Ile 82 Val 171 Met 172	His 54 Gln 55 Arg 140 Arg 142 Gln 143	Gly 53 Tyr 56 Met 70 Tyr 134 Tyr 139 Gly 141 Tyr 144	Cys 54 Gln 55 Arg 140 Arg 142 Gln 143	Gly 53 Tyr 56 Met 70 Tyr 134 Tyr 139 Gly 141 Tyr 144	Glu 135 Arg 142 Arg 163	Tyr 144 Trp 157 Ala 159 Met 160 Asn 161 Ala 162 Val 164	Cys 54 Gln 55 Arg 142 Gln 143	Phe 51 Thr 52 Gly 53 Tyr 144 Gly 158 Met 160
<b>Pocket 22</b>		<b>Pocket 19</b>		<b>Pocket 20</b>		<b>Pocket 18</b>		<b>Pocket 13</b>		<b>Pocket 22</b>	
Cys 42 Ser 81	Met 1 Gly 2 Gly 41	Glu 95 Gln 102 Ser 104	Ile 93 Tyr 94 Phe 117	Cys 109	Met 90 Leu 92 Leu 105	Ser 111 Gln 113 Asn 119	Leu 112 Phe 118 Met 136	Gln 26 Ser 30 Arg 31	Leu 25 Phe 29 Val 75	Cys 42 His 84 Ser 85	Ile 82 Pro 83 Tyr 130

$\gamma$ A-crystallin		$\gamma$ B-crystallin		$\gamma$ C-crystallin		$\gamma$ D-crystallin		$\gamma$ E-crystallin		$\gamma$ F-crystallin	
hydrophilic	hydrophobic	hydrophilic	hydrophobic	hydrophilic	hydrophobic	hydrophilic	hydrophobic	hydrophilic	hydrophobic	hydrophilic	hydrophobic
<b><u>Pocket 18</u></b> Glu 135 Asp 161 Lys 163	Leu 133 Tyr 144 Ala 159	<b><u>Pocket 15</u></b> Glu 47 Ser 73 Ser 75	Tyr 56 Phe 72	<b><u>Pocket 16</u></b> Gln 113 Ser 119 Lys 163	Pro 137 Ala 164 Gly 165	<b><u>Pocket 14</u></b> Thr 52 Gln 55	Phe 51 Gly 53 Tyr 144 Gly 158	<b><u>Pocket 9</u></b> Arg 79 Arg 147 Asp 156	Tyr 45 Leu 145 Tyr 151 Trp 157	<b><u>Pocket 18</u></b> Glu 96 His 122 Arg 153	Tyr 154 Trp 157 Ala 162
<b><u>Pocket 17</u></b> Cys 109 Ser 166	Leu 105 Ile 112 Val 164 Leu 167	<b><u>Pocket 14</u></b> Gln 114 Ser 120	Leu 113 Leu 119 Pro 138 Val 165 Gly 166	<b><u>Pocket 15</u></b> Glu 47 Ser 73 Ser 75	Tyr 56 Trp 69 Phe 72 Ile 76	<b><u>Pocket 13</u></b> Ser 31 Arg 32 Asp 74 Ser 75 Arg 77		<b><u>Pocket 8</u></b> Ser 72 Asp 73 Ser 74	Tyr 55 Trp 68 Val 75	<b><u>Pocket 17</u></b> His 84	Met 1 Gly 2 Gly 41 Leu 81 Ile 82 Pro 83
<b><u>Pocket 16</u></b> His 113 Asn 119 Lys 163	Ile 112 Pro 137 Gly 165	<b><u>Pocket 13</u></b> Gln 84 His 85 Asp 173	Tyr 89 Met 172 Tyr 175	<b><u>Pocket 14</u></b> Gln 55 Arg 147 Asp 156	Tyr 46 Leu 145 Tyr 151 Trp 157	<b><u>Pocket 12</u></b> His 84 His 88 Asp 172	Ala 85 Met 171 Tyr 174	<b><u>Pocket 7</u></b> Glu 46 Cys 53 Ser 72	Tyr 55 Phe 71	<b><u>Pocket 16</u></b> Gln 113 Arg 163	Pro 137 Val 164 Gly 165
<b><u>Pocket 15</u></b>	Ile 121 Met 124 Leu 133 Leu 146 Trp 157	<b><u>Pocket 12</u></b> Arg 80 Arg 148	Ile 82 Pro 83 Leu 146	<b><u>Pocket 13</u></b> Gln 52 Gln 55	Tyr 51 Gly 53 Tyr 144 Gly 158	<b><u>Pocket 11</u></b> Arg 80 Arg 147	Leu 145 Tyr 151	<b><u>Pocket 6</u></b> His 122	Phe 121 Trp 157 Ala 162	<b><u>Pocket 15</u></b> Asp 65 Gln 67 Gln 68	Pro 64

$\gamma$ A-crystallin		$\gamma$ B-crystallin		$\gamma$ C-crystallin		$\gamma$ D-crystallin		$\gamma$ E-crystallin		$\gamma$ F-crystallin	
hydrophilic	hydrophobic	hydrophilic	hydrophobic	hydrophilic	hydrophobic	hydrophilic	hydrophobic	hydrophilic	hydrophobic	hydrophilic	hydrophobic
<b><u>Pocket 14</u></b> Ser 103	Leu 92 Ile 112 Phe 116 Leu 118 Ile 121	<b><u>Pocket 11</u></b> His 85 Cys 131	Pro 83 Tyr 89 Val 171	<b><u>Pocket 12</u></b>	Met 90 Leu 92 Leu 105 Leu 167	<b><u>Pocket 10</u></b>	Ile 4 Val 38 Trp 43 Leu 45 Leu 58	<b><u>Pocket 5</u></b> Ser 85 His 88 Arg 169	Met 171	<b><u>Pocket 14</u></b> Arg 168 Arg 169	Phe 57 Val 132 Tyr 134 Ile 170
<b><u>Pocket 13</u></b> Gln 55 Arg 142 Gln 143	Tyr 54 Tyr 144	<b><u>Pocket 10</u></b> Arg 148 Asp 157	Leu 146 Tyr 152 Trp 158	<b><u>Pocket 11</u></b> Glu 94	Leu 92 Val 101 Met 103 Leu 118	<b><u>Pocket 9</u></b> Glu 47 Ser 75	Leu 45 Tyr 46 Tyr 56 Val 76	<b><u>Pocket 4</u></b> Lys 2 Arg 36 Asp 38	Ile 3 Thr 4	<b><u>Pocket 13</u></b> Ser 73 Asp 74	Cys 33 Trp 69 Val 76
<b><u>Pocket 12</u></b> Cys 42 Arg 59 Arg 60 Asp 172	Gly 41	<b><u>Pocket 9</u></b> Glu 121	Leu 113 Leu 119 Ile 122 Val 165	<b><u>Pocket 10</u></b> Lys 163	Leu 133 Trp 157 Ala 162 Ala 164	<b><u>Pocket 8</u></b> Arg 59 Arg 168 Arg 168	Met 171	<b><u>Pocket 3</u></b> Ser 72 Ser 74	Tyr 55	<b><u>Pocket 12</u></b> Glu 47 Cys 54 Ser 73	Tyr 54 Tyr 56 Phe 72
<b><u>Pocket 11</u></b> Ser 86 His 88 Arg 169	Met 171	<b><u>Pocket 8</u></b> Arg 15 Cys 16	Tyr 29 Phe 30	<b><u>Pocket 9</u></b> Arg 168	Met 70 Tyr 134 Tyr 139	<b><u>Pocket 7</u></b> Arg 59 Arg 168 Arg 169	Phe 57 Met 171	<b><u>Pocket 2</u></b>	Leu 133 Tyr 134 Tyr 144 Val 164	<b><u>Pocket 11</u></b> Asn 161 Arg 163	Tyr 144 Trp 157 Ala 159

$\gamma$ A-crystallin		$\gamma$ B-crystallin		$\gamma$ C-crystallin		$\gamma$ D-crystallin		$\gamma$ E-crystallin		$\gamma$ F-crystallin	
hydrophilic	hydrophobic	hydrophilic	hydrophobic	hydrophilic	hydrophobic	hydrophilic	hydrophobic	hydrophilic	hydrophobic	hydrophilic	hydrophobic
<b><u>Pocket 10</u></b> Thr 85 Ser 87 His 88 Glu 128	Glv 129	<b><u>Pocket 7</u></b> Glu 95 Glu 121	Tyr 94 Leu 119 Ile 122	<b><u>Pocket 8</u></b> Gln 143	Phe 57 Trp 69 Met 70	<b><u>Pocket 6</u></b> Gln 27 Arg 77	Leu 26 Phe 30 Val 76	<b><u>Pocket 1</u></b> Glu 46 Ser 72 Ser 74	Tvr 55	<b><u>Pocket 10</u></b> Ser 73 Ser 75	Tvr 56 Trp 69 Val 76
<b><u>Pocket 9</u></b> Glu 47 Ser 73 Ser 75	Tyr 56 Trp 69 Ile 76	<b><u>Pocket 6</u></b> Ser 73 Ser 75	Tyr 56 Trp 69 Ile 76	<b><u>Pocket 7</u></b> Arg 15 Cys 16	Tyr 29 Phe 30	<b><u>Pocket 5</u></b> Arg 15	Pro 28 Tyr 29			<b><u>Pocket 9</u></b> Ser 86 Ser 87 His 88 Arg 169	Met 171
<b><u>Pocket 8</u></b>	Ile 90 Leu 105 Trp 131 Leu 167	<b><u>Pocket 5</u></b>	Ile 93 Tyr 94 Leu 119 Ile 122	<b><u>Pocket 6</u></b> Arg 91	Met 90 Leu 92 Leu 105	<b><u>Pocket 4</u></b>	Met 1 Leu 81 Pro 83			<b><u>Pocket 8</u></b> Lvs 3 Thr 5 Arg 37 Asp 39	Ile 4
<b><u>Pocket 7</u></b> Arg 153	Tyr 122 Tyr 154	<b><u>Pocket 4</u></b> Glu 95 Glu 121	Leu 119	<b><u>Pocket 5</u></b> Ser 87 Arg 89 Ser 106		<b><u>Pocket 3</u></b> Arg 15 His 16	Tyr 29 Phe 30			<b><u>Pocket 7</u></b> Arg 59 Arg 168	Met 171 Tyr 173
<b><u>Pocket 6</u></b> Arg 91 His 125	Tyr 93	<b><u>Pocket 3</u></b> Cys 42 Arg 59 Arg 60 Asp 173	Gly 41	<b><u>Pocket 4</u></b>	Tyr 93 Leu 118 Val 121	<b><u>Pocket 2</u></b> Thr 5 Arg 37 Asp 39				<b><u>Pocket 6</u></b> Arg 15 His 16	Tyr 17 Tyr 29 Phe 30

$\gamma$ A-crystallin		$\gamma$ B-crystallin		$\gamma$ C-crystallin		$\gamma$ D-crystallin		$\gamma$ E-crystallin		$\gamma$ F-crystallin	
hydrophilic	hydrophobic	hydrophilic	hydrophobic	hydrophilic	hydrophobic	hydrophilic	hydrophobic	hydrophilic	hydrophobic	hydrophilic	hydrophobic
<b><u>Pocket 5</u></b> Ser 87 His 88 Arg 89 Thr 106		<b><u>Pocket 2</u></b> Gln 144	Phe 57 Trp 69	<b><u>Pocket 3</u></b> His 84 Cys 130	Pro 83 Val 170	<b><u>Pocket 1</u></b> Gln 143	Phe 57 Trp 69			<b><u>Pocket 5</u></b> His 80 Arg 147	Tyr 46 Phe 51
<b><u>Pocket 4</u></b> Gln 143	Phe 57 Trp 69 Met 70	<b><u>Pocket 1</u></b> Lys 3 Glu 18 Cys 19 Ser 20		<b><u>Pocket 2</u></b> Glu 94	Tyr 93 Leu 118 Val 121					<b><u>Pocket 4</u></b> Ser 73 Ser 75	Tyr 56
<b><u>Pocket 3</u></b> Arg 142	Gly 53 Tyr 54 Tyr 144			<b><u>Pocket 1</u></b> Cys 42 Arg 59	Gly 41					<b><u>Pocket 3</u></b> Arg 59 Arg 168	Phe 57 Met 171
<b><u>Pocket 2</u></b> Asp 172	Tyr 84 Met 171 Tyr 174									<b><u>Pocket 2</u></b> His 155	Tyr 154 Met 160
<b><u>Pocket 1</u></b> Cys 42 Ser 81	Gly 41 Trp 143									<b><u>Pocket 1</u></b> Arg 147	Leu 145

Table 3: Comparison of the binding pockets for their ligand (aspirin, fructose, glucose, ibuprofen, Vitamin C)

Receptor	Aspirin	Fructose	Glucose	Ibuprofen	Vitamin C
$\gamma$ A-crystallin	P23 (4) P21 (2) P20 (2) P19 (1) P4 (1)	P23 (8)  P20 (2)	P23 (6) P22 (1) P20 (2) P2 (1)	P23 (6)  P20 (4)	P23 (7) P22 (1) P20 (2)
$\gamma$ B-crystallin	P18 (1) P16 (6) P10 (2) P2 (1)	P21 (2) P12 (2) P10 (1) P2 (5)	P21 (1) P16 (2) P10 (2) P2 (4)	 P16 (3) P3 (7)	P21 (1) P20 (1) P18 (2) P13 (1) P10 (2) P2 (3)
$\gamma$ C-crystallin	P21 (2) P14 (4) P9 (3)	P21 (6) P20 (1) P9 (3)	P22 (1) P21 (4) P14 (2)	P21 (1) P14 (2) P9 (2)	P21 (2) P20 (1) P14 (5) P9 (1)
$\gamma$ D-crystallin	P19 (1) P18 (1) P1 (8)	P19 (4) P11 (1) P7 (1) P1 (4)	P19 (3) P18 (6)	P19 (4) P1 (6)	P20 (1) P19 (1) P18 (2) P4 (1) P1 (5)
$\gamma$ E-crystallin	P15 (1) P14 (1) P12 (3) P11 (3) P9 (2)	P15 (4) P14 (1) P12 (1) P11 (2) P9 (2)	P15 (2) P14 (1) P12 (1) P11 (2) P9 (3) P5 (1)	P12 (4) P11 (1) P9 (5)	P15 (4) P12 (2) P11 (3) P9 (1)
$\gamma$ F-crystallin	P24 (1) P23 (5) P20 (1) P17 (3)	P23 (1) P17 (4) P18 (5)	P24 (2) P23 (1) P22 (3) P17 (1) P16 (3)	P24 (5) P22 (2) P20 (2) P17 (1)	P24 (4) P22 (2) P16 (4)

Numbers in brackets represent the number of poses  
P stands for pocket

Table 4: Results of the fructose ligand docking. The energy values are given in kcal/mol

receptor	Binding Energy	Ki ( $\mu$ M)	Intermolecular energy	Pocket Volume ( $\text{\AA}^3$ )	Residues involved in close contact
$\gamma$ A-Cryst	-6.06	35.99	-6.66	5H	<b>Y46</b> , N50, Y51, Q55, <b>R80</b> , Y144, <b>L145</b> , L146, <b>R147</b> , <b>Y151</b> , D156, W157, G158 <i>Pose II (P23)</i>
$\gamma$ B-Cryst	-5.13	172.71	-5.73	4H	H54, <b>Q55</b> , Y56, W69, <b>M70</b> , G71, F72, R141, G142, R143, <b>Q144</b> <i>Pose I (P21)</i>
$\gamma$ C-Cryst	-5.41	108.37	-6.01	5H	<b>H54</b> , <b>Q55</b> , <b>Y56</b> , M70, G71, F72, G141, R142, <b>Q143</b> <i>Pose V (P21)</i>
$\gamma$ D-Cryst	-5.19	156.64	-5.79	7H	Y56, <b>F57</b> , L58, <b>R59</b> , W69, M70, <b>Y134</b> , Y139, Q143, <b>R168</b> <i>Pose I (P1)</i>
$\gamma$ E-Cryst	-5.17	163.3	-5.72	6H	<b>Y45</b> , F50, <b>Q54</b> , <b>R79</b> , Y144, L145, L146, <b>R147</b> , Y151, D156, <b>W157</b> , G158 <i>Pose VI (P9)</i>
$\gamma$ F-Cryst	-4.81	298.07	-5.41	4H	<b>M1</b> , G2, S40, G41, <b>C42</b> , L81, <b>I82</b> , P83, <b>H84</b> , S85, I170, M171, D172 <i>Pose IX (P17)</i>

Hydrogen bonded residues are highlighted in bold.

Table 5: Results of the glucose ligand docking. The energy values are given in kcal/mol

Receptor	Binding Energy	Ki ( $\mu\text{M}$ )	Intermolecular energy	Pocket Volume ( $\text{\AA}^3$ )	Residues involved in close contact
$\gamma\text{A-Cryst}$	-3.68	2000	-5.47	3H	Y56, <b>F57</b> , L58, Y63, <b>Q68</b> , W69, M70, <b>Y134</b> , Y139, Q143, R168 <i>Pose V (P20)</i>
$\gamma\text{B-Cryst}$	-4.17	879.92	-5.96	8H	Y56, <b>F57</b> , L58, Y63, <b>Q68</b> , W69, M70, <b>Y135</b> , <b>Y140</b> , R141, <b>Q144</b> , <b>R169</b> <i>Pose III (P21)</i>
$\gamma\text{C-Cryst}$	-3.94	1290	-5.73	5H	R59, R60, G61, <b>D62</b> , <b>Y63</b> , P64, <b>Q68</b> , W69, M70 <i>Pose V (P )</i>
$\gamma\text{D-Cryst}$	-5.27	137.43	-7.06	5H	S111, L112, <b>Q113</b> , F118, N119, <b>E135</b> , M136, <b>T137</b> , <b>R163</b> , V164, G165 <i>Pose I (P18)</i>
$\gamma\text{E-Cryst}$	-4.15	906.66	-5.94	4H	F56, L57, R58, <b>Y62</b> , <b>Q67</b> , W68, M69, <b>Y134</b> , Q143, R168, F173 <i>Pose I (P12)</i>
$\gamma\text{F-Cryst}$	-4.31	698.44	-6.10	4H	Y56, F57, L58, <b>R59</b> , Y63, Q68, W69, M70, V132, <b>Y134</b> , Y139, <b>Q143</b> , <b>R168</b> <i>Pose X (P24)</i>

Hydrogen bonded residues are highlighted in bold.

Table 6: Results of the aspirin ligand docking. The energy values are given in kcal/mol

Receptor	Binding energy	Ki ( $\mu$ M)	Intermolecular energy	Pocket Volume ( $\text{\AA}^3$ )	Residues involved in close contact
$\gamma$ A-cryst	-5.72	64.15	-6.91	3H	Y46, Y51, Q52, Q55, <b>R80</b> , Y144, L145, L146, R147, <b>Y151</b> , D156, W157, G158 <i>Pose I (P23)</i>
$\gamma$ B-cryst	-6.32	23.44	-7.51	3H	Y46, N50, Y51, Q52, G53, Q55, <b>R80</b> , Y145, L146, <b>R148</b> , D157, W158, G159 <i>Pose VII (P16)</i>
$\gamma$ C-cryst	- 6.27	25.36	-7.46	4H	Y46, N50, Y51, Q52, <b>Q55</b> , <b>R80</b> , Y144, L145, <b>R147</b> , Y151, D156, W157, G158 <i>Pose I (P14)</i>
$\gamma$ D-cryst	-5.79	56.55	-6.99	4H	F57, L58, <b>R59</b> , R60, G61, <b>Y63</b> , Q68, W69, M70, Y134, Q143, R168, 173 <i>Pose I (P 1)</i>
$\gamma$ E-cryst	-5.90	47.01	-7.1	4H	G40, C41, I81, P82, <b>H83</b> , <b>S84</b> , H88, Y130, I170, M171, <b>D172</b> <i>Pose I (P11)</i>
$\gamma$ F-cryst	-5.34	122.11	-6.53	2H	T52, G53, C54, <b>Q55</b> , <b>R142</b> , Q143, Y144, G158, A159, M160, N161 <i>Pose III (P23)</i>

Hydrogen bonded residues are highlighted in bold.

Table 7: Results of the ibuprofen ligand docking. The energy values are given in kcal/mol

Receptor	Binding Energy	Ki ( $\mu\text{M}$ )	Intermolecular energy	Pocket Volume ( $\text{\AA}^3$ )	Residues involved in close contact
$\gamma\text{A-Cryst}$	-6.33	22.95	-7.82	3H	Y46, Y51, Q52, G53, Q55, <b>R80</b> , Y144, L145, <b>R147</b> , Y151, G158 <i>Pose II (P23)</i>
$\gamma\text{B-Cryst}$	-5.57	83.32	-7.06	1H	F57, R59, R60, Y63, M70, Y135, Y140, Q144, <b>R169</b> <i>Pose VI (P21)</i>
$\gamma\text{C-Cryst}$	-6.36	21.76	-7.85	2H	H54, <b>Q55</b> , Y56, M70, G71, F72, G141, R142, <b>Q143</b> <i>Pose IV (P21)</i>
$\gamma\text{D-Cryst}$	-6.05	36.93	-7.54	2H	C54, <b>Q55</b> , Y56, M70, G71, F72, G141, R142, <b>Q143</b> <i>Pose X (P19)</i>
$\gamma\text{E-Cryst}$	-4.99	218.97	-6.48	1H	F56, L57, R58, Y62, Q67, W68, M69, Y134, N138, Y139, R140, Q143, <b>R168</b> , F173 <i>Pose V (P12)</i>
$\gamma\text{F-Cryst}$	-6.75	11.27	-8.24	2H	F57, L58, <b>R59</b> , R60, G61, D62, Y63, Q68, W69, M70, Y134, Y139, Q143, <b>R168</b> , Y173, Y174 <i>Pose I (P24)</i>

Hydrogen bonded residues are highlighted in bold.

Table 8: Results of the aspirin ligand docking. The energy values are given in kcal/mol

Receptor	Binding Energy	Ki ( $\mu$ M)	Intermolecular energy	Pocket Volume ( $\text{\AA}^3$ )	Residues involved in close contact
$\gamma$ A-Cryst	5.05	199.95	-6.84	6H	Y46, <b>Y51</b> , Q52, Q55, <b>R80</b> , Y144, <b>L145</b> , L146, <b>R147</b> , <b>Y151</b> , W157, G158 <i>Pose VII (P23)</i>
$\gamma$ B-Cryst	-4.63	404.59	-6.42	5H	<b>Y46</b> , <b>N50</b> , Y51, Q52, Q55, <b>R80</b> , Y145, <b>L146</b> , L147, <b>R148</b> , Y152, D157, W158, G159 <i>Pose II (P16)</i>
$\gamma$ C-Cryst	-5.52	90.66	-7.3	7H	<b>Y46</b> , <b>N50</b> , Y51, Q52, Q55, <b>R80</b> , Y144, <b>L145</b> , <b>R147</b> , D156, <b>W157</b> , G158 <i>Pose VII (P14)</i>
$\gamma$ D-Cryst	-4.66	386.9	-6.45	4H	Y56, <b>F57</b> , L58, <b>R59</b> , Y63, Q68, W69, M70, Y134, <b>Q143</b> , R168, F173 <i>Pose V (P1)</i>
$\gamma$ E-Cryst	-3.43	3090	-5.21	3H	Y55, <b>F56</b> , L57, Q67, W68, M69, <b>Y134</b> , N138, <b>Y139</b> , R140, Q143, R168 <i>Pose VIII (P12)</i>
$\gamma$ F-Cryst	-3.86	1490	-5.65	5H	F57, L58, <b>R59</b> , R60, G61, <b>D62</b> , <b>Y63</b> , Q68, W69, <b>Y174</b> <i>Pose I (P24)</i>

Hydrogen bonded residues are highlighted in bold.

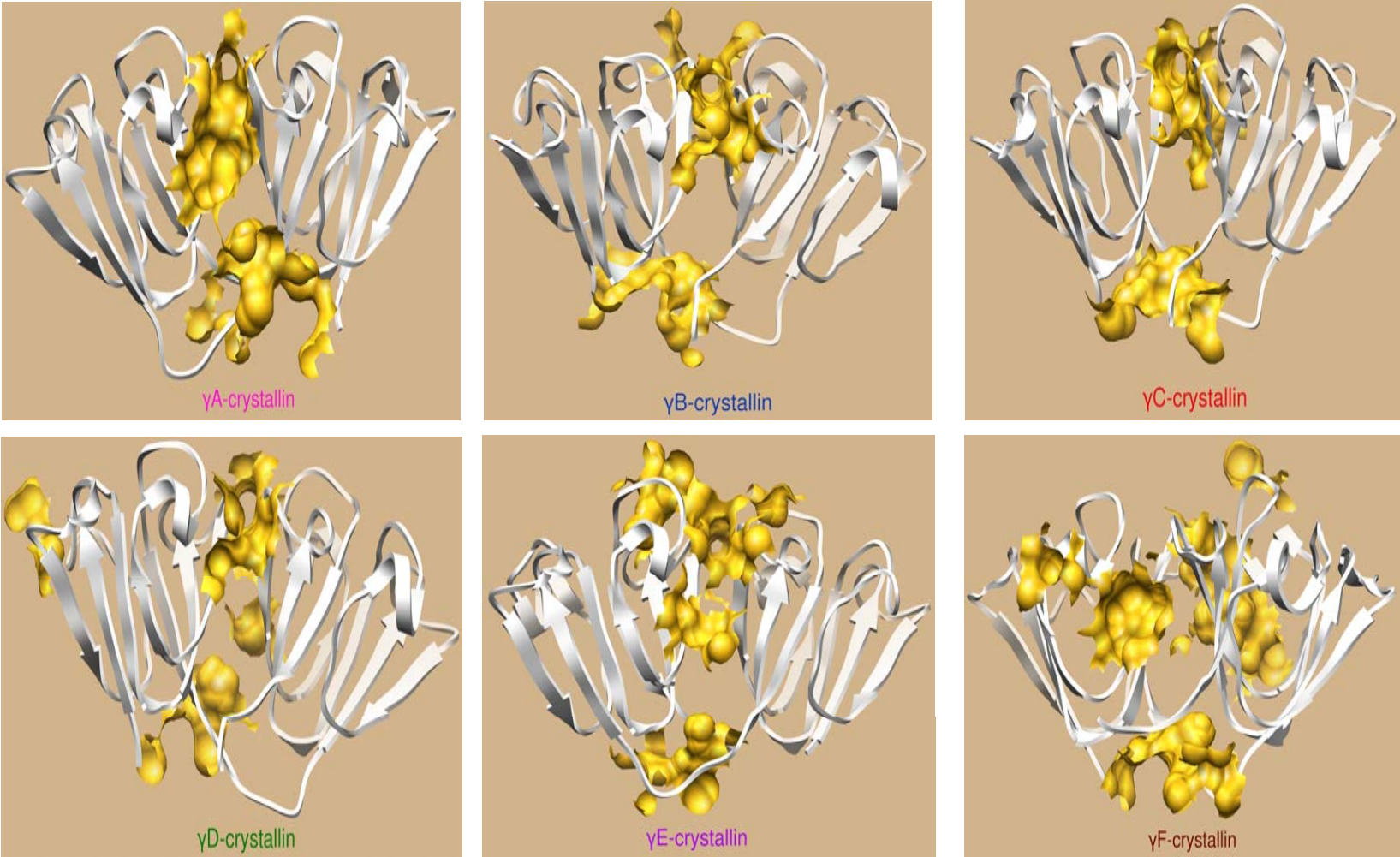


Figure 1: Ribbon representation of the  $\gamma$ -crystallin proteins showing the regions that form the contiguous binding sites



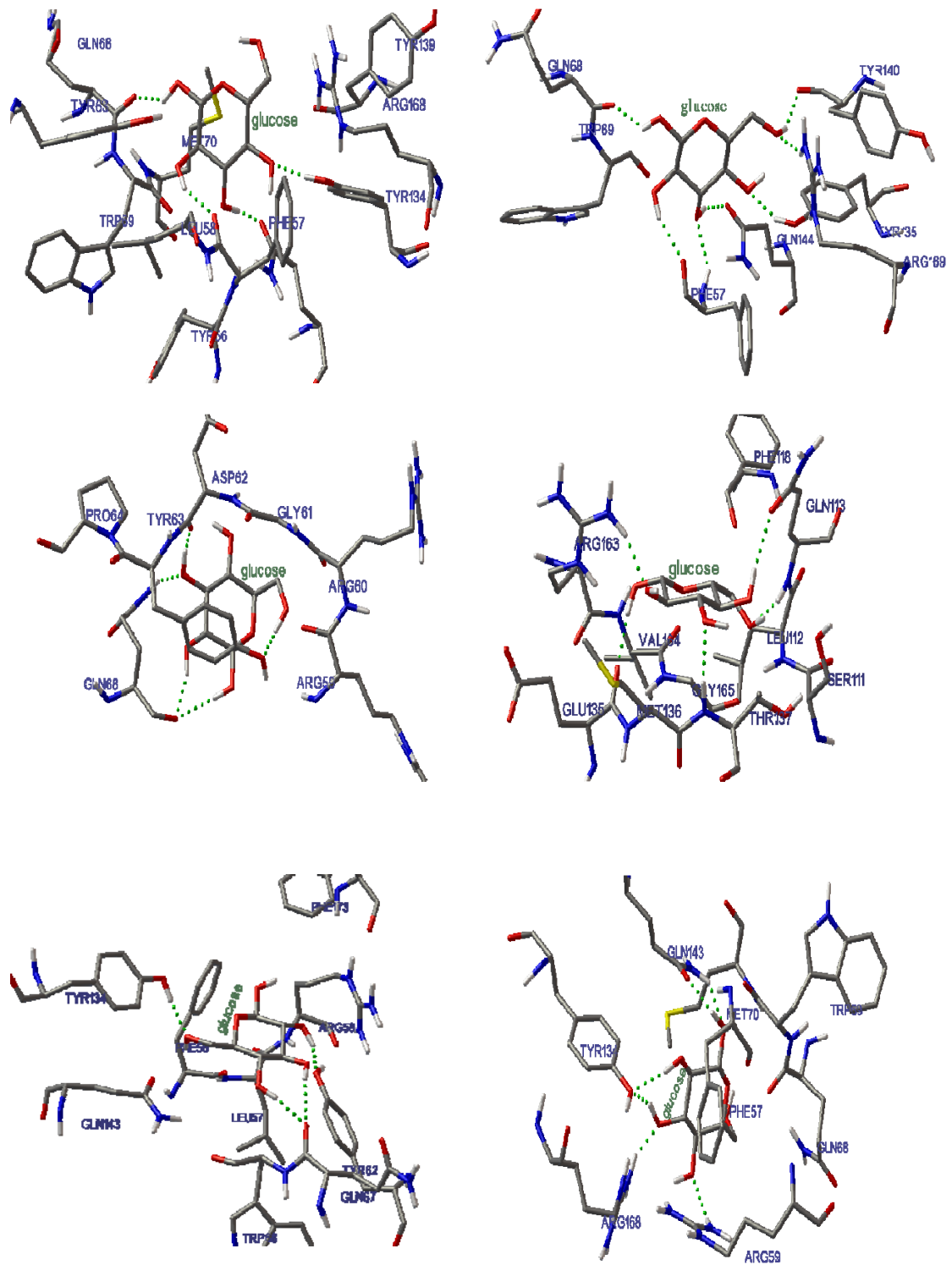


Figure 3: Molecular Interaction of glucose with the individual members of rat  $\gamma$ -crytallin family. Hydrogen bonds are indicated as green dotted lines.

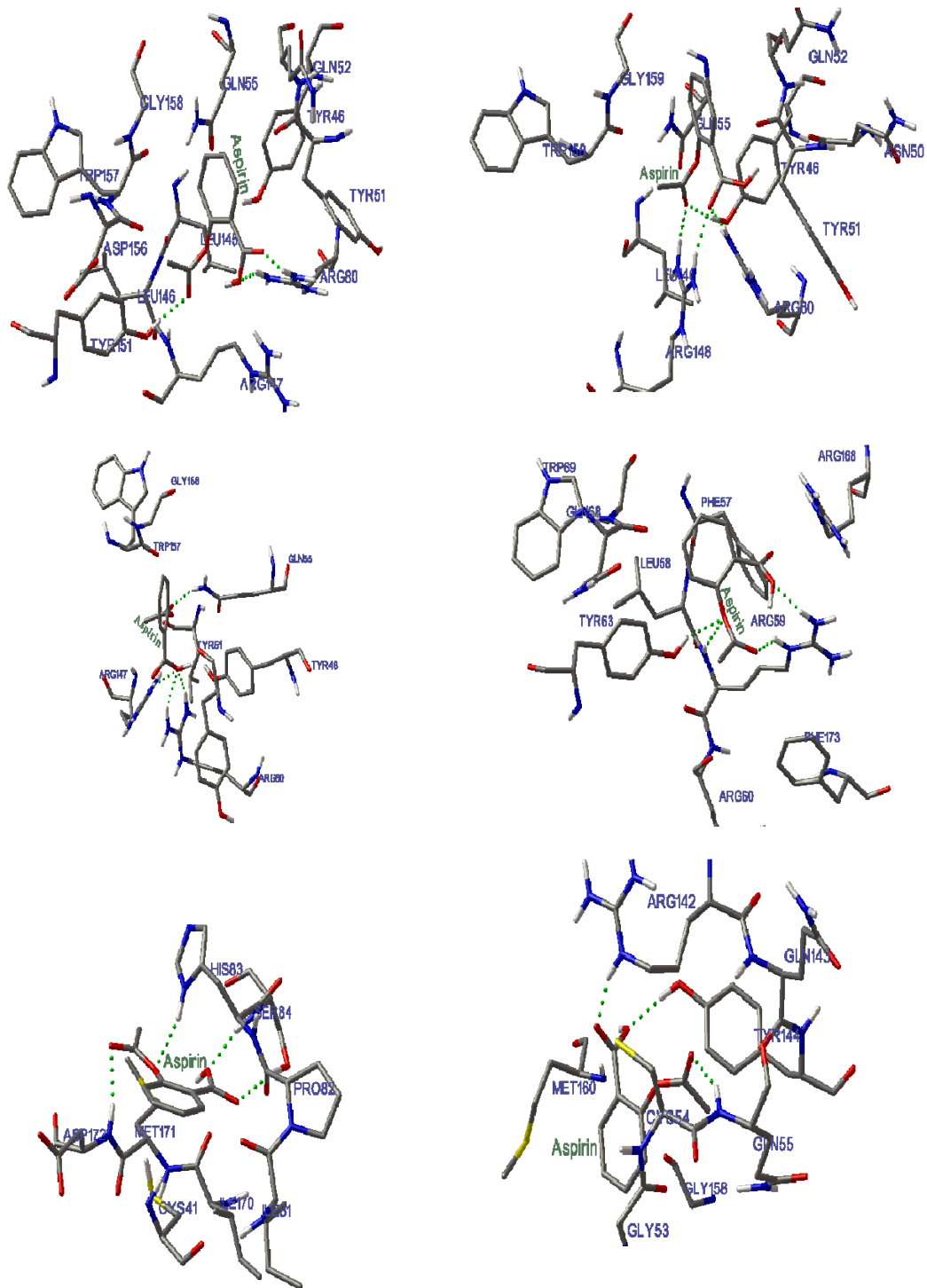


Figure 4: Molecular Interaction of aspirin with the individual members of rat  $\gamma$ -crystallin family. Hydrogen bonds are indicated as green dotted lines.

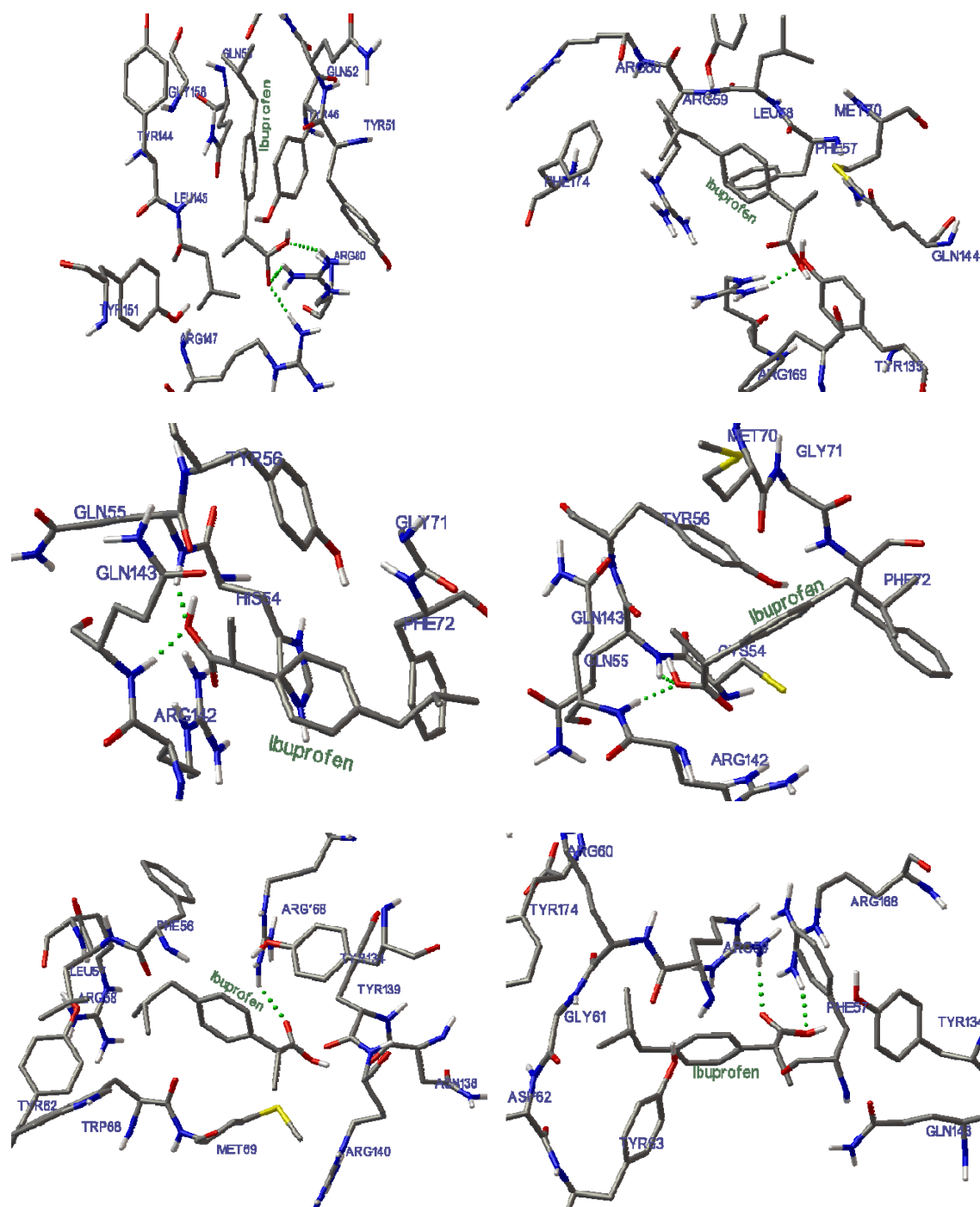


Figure 5: Molecular Interaction of ibuprofen with the individual members of rat  $\gamma$ -crytallin family. Hydrogen bonds are indicated as green dotted lines.

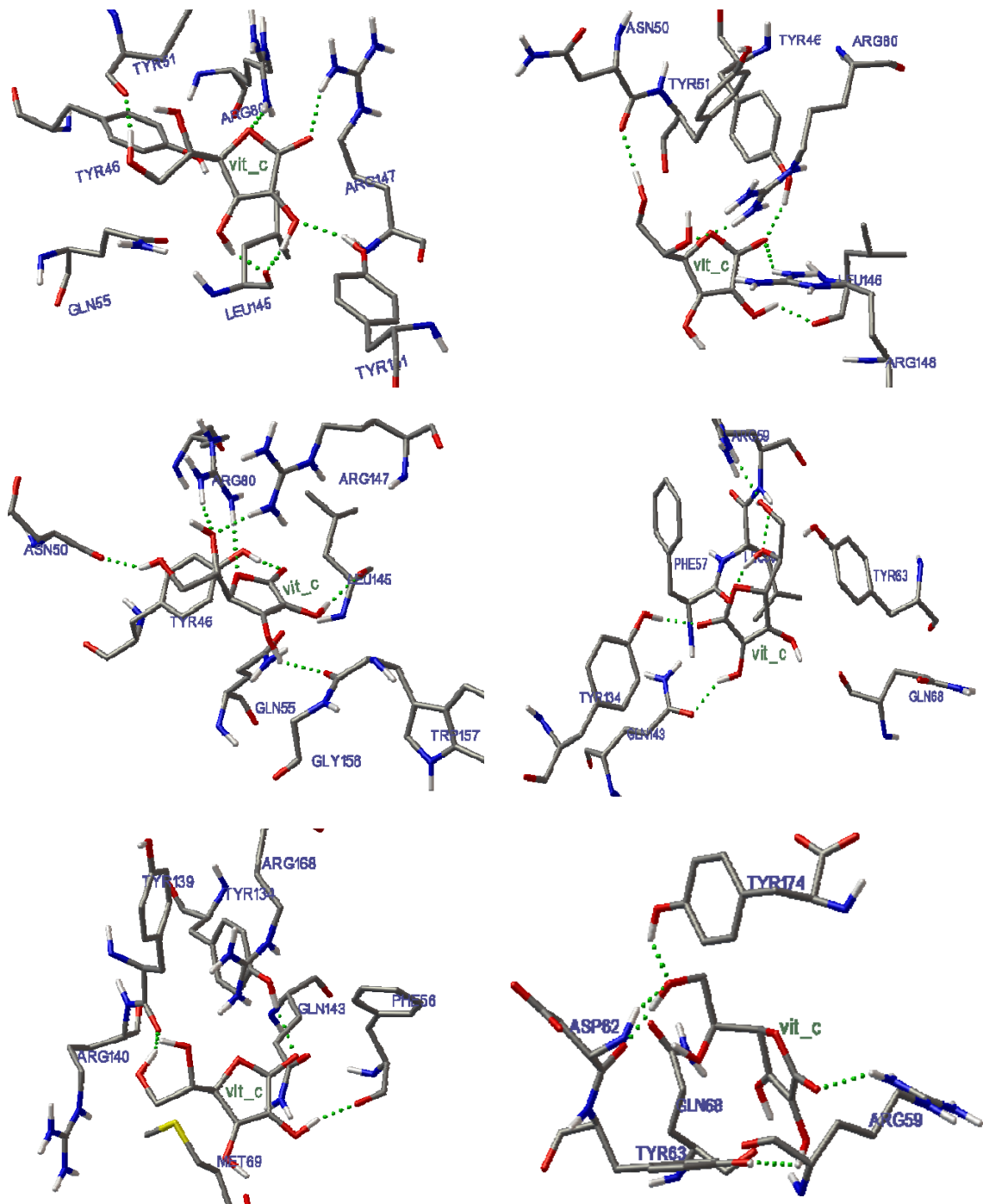


Figure 6: Molecular Interaction of vitamin-C with the individual members of rat  $\gamma$ -crystallin family. Hydrogen bonds are indicated as green dotted lines.

## 5 Conclusion

In conclusion, the results suggested that experimental and computational methods could be used to predict the binding sites of rat  $\gamma$ -crystallin family. These binding sites can be used to explore small ligands binding onto  $\gamma$ -crystallin family and modulate and/or inhibit their function and to facilitate the design of new drug candidates for cataract.

## References

- [1] G. Wistow and J. Piatigorsky, Lens crystallins: The evolution and the expression of protein for a highly specialized tissue, *Ann. Rev. Biochem.*, **57**, (1988), 479-504.
- [2] P.R. Ocken, S.C. Fu, R. Hart, J.H. White, B.J. Wagner, K.E. Lewis, Characterization of lens proteins I. Identification of additional soluble fractions in rat lenses, *Exp. Eye Res.*, **24**, (1977), 355-367.
- [3] E. Wada, T. Sugiura, H. Nakamura and T. Tsumita, Studies on lens proteins of mice with hereditary cataract. I. Comparative studies on the chemical and immunochemical properties of the soluble proteins of cataractous and normal mouse lenses, *Biochim. Biophys. Acta.*, **667**, (1981), 251-259.
- [4] H. Bloemendal, W. de Jong, R. Jaenicke, N.H. Lubsen, C. Slingsby, A. Tardieu, Ageing and vision: structure, stability and function of lens crystallins, *Prog Biophys. Mol. Biol.*, **86**, (2004), 407-485.
- [5] G. D'Alessio, The evolution of monomeric and oligomeric betagamma-type crystallins. Facts and hypotheses, *Eur J Biochem*, **269**, (2002), 3122-3130.
- [6] A.A. Gawad, Homology modelling of rat  $\gamma$ -crystallins: I. Electrostatic surface properties, *J. Biophys. Biomed. Sci.*, **2**, (2009), 152-159.
- [7] R. Vornhagen, J. Bours and H. Rink, Immunological properties of rat lens gamma-crystallins, I. Characterization of the major components, *Ophthalmic*

- Res.*, **14**, (1982), 298-304.
- [8] R.J. Siezen, E. Wu, E.D. Kaplan, J.A. Thomson and G.B. Benedek, Rat lens gamma-crystallins. Characterization of the six gene products and their spatial and temporal distribution resulting from differential synthesis, *J. Mol. Biol.*, **199**, (1988), 475-490.
- [9] X. Wang, C.M. Garcia, Y.B. Shui and D.C. Beebe, Expression and regulation of  $\alpha$ -,  $\beta$ -, and  $\gamma$ -crystallins in mammalian lens epithelial cells, *Invest. Ophthalmol. Vis. Sci.*, **45**, (2004), 3608-3619.
- [10] D. Sinha, N. Esumi, C. Jaworski, C.A. Kozak, E. Pierce and G. Wistow, Cloning and mapping the mouse crygs gene and non-lens expression of  $\gamma$ -crystallin, *Mol. Vis.*, **4**, (1998), 8-15.
- [11] S.E. Jones, C. Jomary, J. Grist, J. Makwana, and M.J. Neal, Retinal expression of  $\gamma$ -crystallins in the mouse, *Invest. Ophthalmol. Vis. Sci.*, **40**, (1999), 3017-3020.
- [12] J. Xi, R. Farjo, S. Yoshida, T.S. Kern, A. Swaroop, U.P. Andley, A comprehensive analysis of the expression of crystallins in mouse retina, *Mol. Vis.*, **9**, (2003), 410-419.
- [13] C. Slingsby and N. J. Clout, Structure of the crystallins, *Eye*, **13**, (1999), 395-402.
- [14] Z. Ma, S.R. Hanson, K.J. Lampi, L.L. David, D.L. Smith, J.B. Smith, Age-related changes in human lens crystallins identified by HPLC and mass spectrometry, *Exp Eye Res*, **67**, (1998), 21-30.
- [15] A. Pande, K.S. Ghosh, P.R. Banerjee and J. Pande, Increase in surface hydrophobicity of the cataract-associated P23T mutant of human gammaD-crystallin is responsible for its dramatically lower, retrograde solubility, *Biochemistry*, **49**, (2010), 6122-6129.
- [16] M. Sakthivel, R. Elanchezian, P.A. Thomas and P. Geraldine, Alterations in lenticular proteins during ageing and selenite-induced cataractogenesis in Wistar rats, *Mol. Vis.*, **16**, (2010), 445-53.

- [17] J. Fan, A.K. Donovan, D.R. Ledee, P.S. Zelenka, R.N. Fariss and A.B. Chepelinsky,  $\gamma$ E-crystallin recruitment to the plasma membrane by specific interaction between lens MIP/aquaporin-0 and  $\gamma$ E-crystallin, *Invest. Ophthalmol. Vis. Sci.*, **45**, (2004), 863-871.
- [18] J. Piatigorsky, Multifunctional lens crystallins and corneal enzymes. More than meets the eye, *Ann N Y Acad Sci.*, **842**(15), (1998), 7-15.
- [19] U.P. Andley, Crystallins in the eye: Function and pathology, *Prog. Retin. Eye Res.*, **26**, (2007), 78-98.
- [20] J. Horwitz, Alpha-crystallin, *Exp Eye Res*, **76**, (2003), 145-153.
- [21] J. Graw, The genetic and molecular basis of congenital eye defects, *Nat Rev Genet*, **4**, (2003), 876-888.
- [22] N. Eswar, N. John, N. Mirkovic, A. Fiser, VA Ilyin, U. Pieper, AC Stuart, MA Marti-Renom, MS Madhusudhan, B Yerkovich, et al., Tools for comparative protein structure modeling and analysis, *Nucleic Acids Res*, **31**, (2003), 3375-3380.
- [23] A. Sali and T.L. Blundell, Comparative protein modelling by satisfaction of spatial restraints, *J Mol Biol*, **234**, (1993), 779-815.
- [24] J. Dundas, Z. Ouyang, J. Tseng, A. Binkowski, Y. Turpaz, J. Liang, CASTp: computed atlas of surface topography of proteins with structural and topographical mapping of functionally annotated residues, *Nucl Acids Res*, **34**, (2006), W116-8.
- [25] A.T.R Laurie and R.M. Jackson, Q-SiteFinder: an energy-based method for the prediction of protein–ligand binding sites, *Bioinformatics*, **21**, (2005), 1908-1916.
- [26] G.M. Morris, D.S. Goodsell, R.S. Halliday, R. Huey, W. E. Hart, R.K. Belew, A.J. Olson, Automated docking using a Lamarckian genetic algorithm and an empirical binding free energy function, *J. Comput Chem*, **19**, (1998), 1639-1662.

- [27] C. Hetényi and D. van der Spoel, Efficient docking of peptides to proteins without prior knowledge of the binding site, *Protein Sci*, **11**, (2002), 1729-1737.
- [28] R. Huey, G.M. Morris, A.J. Olson, and D.S. Goodsell, A semiempirical free energy force field with charge-based desolvation, *J. Comput Chem*, **28**, (2006), 1145-1152.
- [29] T.A. Binkowski, S. Naghibzadeh and J. Liang, CASTp: computed atlas of surface topography of proteins, *Nucleic Acids Res*, **31**, (2003), 3352-3355.
- [30] R.A. Laskowski, J.M. Thornton, C. Humblet, J. Singh, X-SITE: use of empirically derived atomic packing preferences to identify favourable interaction regions in the binding sites of proteins, *J. Mol Biol*, **259**, (1996), 175-201.
- [31] J. Liang, H. Edelsbrunner, C. Woodward, Anatomy of protein pockets and cavities: measurement of binding site geometry and implications for ligand design, *Protein Sci*, **7**, (1998), 1884-1897.
- [32] A. Kahraman, R. J. Morris, R.A. Laskowski, J.M. Thornton, Shape variation in protein binding pockets and their ligands, *J. Mol Biol*, **368**, (2007), 283-301.
- [33] V.M. Monnier and A. Cerami, Nonenzymatic glycosylation and browning in diabetes and aging, *Diabetes*, **31**(Suppl. 3), (1982), 57-63.
- [34] T.J. Lyons, G. Silvestri, J.A. Dunn and J.W. Baynes, Role of glycation in modification of lens crystallins in diabetic and nondiabetic senile cataracts, *Diabetes*, **40**, (1991), 1010-1015.
- [35] S. Lal, B.S. Szwegold, A.H. Taylor, W.C. Randall, F. Kappler, K. Wells-Knecht, J.W. Baynes and T.R. Brown, Metabolism of fructose-3-phosphate in the diabetic rat lens, *Arch Biochem Biophys*, **318**, (1995), 191-199.

- [36] J.B. Smith, S.R.A. Hanson, R.L. Cerny, H.R. Zhao and E.C. Abraham, Identification of the glycation site of lens  $\gamma$ B-crystallin by fast atom bombardment tandem mass spectrometry, *Anal Biochem*, **243**, (1996), 186-189.
- [37] H. Yan, Y. Gou, J. Zhang, Z.H. Ding, W.J. Ha and J.J. Harding, Inhibition of cataracts in diabetic rats by carnosine, aminoguanidine and aspirin drops, *Mol Vis*, **14**, (2008), 2282-2291.
- [38] N.F. Brás, P.A. Fernandes and M.J. Ramos, Docking and molecular dynamics studies on the stereoselectivity in the enzymatic synthesis of carbohydrates, *Theor Chem Account*, **122**, (2009), 283-296.
- [39] S. Leis, S. Schneider and M. Zacharias, *In Silico* prediction of binding sites on proteins, *Curr Med Chem*, **17**, (2010), 1550-1562.
- [40] Y. Kawasaki, J. Fujii, N. Miyazawa, A. Hoshi, A. Okado, Y. Tano and N. Taniguchi, Specific detection of the early process of the glycation reaction by fructose and glucose in diabetic rat lens, *FEBS Lett*, **441**, (1998), 116-120.
- [41] M.S. Swamy and E.C. Abraham, Differential glycation of rat  $\alpha$ -,  $\beta$ - and  $\gamma$ -crystallins, *Exp Eye Res*, **52**, (1991), 439-444.
- [42] K.W. Lee, V. Mossine and B.J. Ortwerth, The relative ability of glucose and ascorbate to glycate and crosslink lens proteins in vitro, *Exp Eye Res*, **67**, (1998), 95-104.
- [43] A.Z. Shyadehi and J.J. Harding, Investigations of ibuprofen and paracetamol binding to lens proteins to explore their protective role against cataract, *Biochem Pharmacol*, **42**, (1991), 2077-2084.
- [44] R. Ajiboye and J.J. Harding, The non-enzymic glycosylation of bovine lens proteins by glucosamine and its inhibition by aspirin, ibuprofen and glutathione, *Exp Eye Res*, **49**, (1989), 31-41.
- [45] K.A. Roberts and J.J. Harding, Ibuprofen, a putative anti-cataract drug, protects the lens against cyanate and galactose, *Exp Eye Res*, **50**, (1990), 157-164.

- [46] Q. Shi, H. Yan, M.Y. Li and J.J. Harding, Effect of a combination of carnosine and aspirin eye drops on streptozotocin-induced diabetic cataract in rats, *Mol Vis*, **15**, (2009), 2129-2138.